Cement & Concrete Composites 37 (2013) 293–303

Contents lists available at SciVerse ScienceDirect

Cement & Concrete Composites

journal homepage: www.elsevier.com/locate/cemconcomp

Influence of air entraining agents on deicing salt scaling resistance and transport properties of high-volume fly ash concrete

P. Van den Heede, J. Furniere, N. De Belie *

Magnel Laboratory for Concrete Research, Ghent University, Technologiepark Zwijnaarde 904, B-9052 Ghent, Belgium

ARTICLE INFO

Article history:
Received 14 November 2012
Received in revised form 5 January 2013
Accepted 10 January 2013
Available online 18 January 2013

Keywords:
Deicing salt scaling resistance
Air void analysis
Thin sections
Water penetrability
Gas permeability

ABSTRACT

Based on laboratory tests, the deicing salt scaling resistance of high-volume fly ash (HVFA) concrete is usually reported as less than satisfactory. Therefore, we developed a HVFA composition with an air entraining agent (AEA) that should meet the European salt scaling criterion ($\leqslant$1 kg/m^2). This paper presents a full characterization of its air void system from the moment of casting until the freeze/thaw test on cast surfaces, and evaluates the influence of air entrainment on its transport properties. The minimum air content of 6–7% was achieved with 7.0 ml AEA/kg binder (versus 2.0 ml AEA/kg binder for traditional concrete). However, with very fine fly ash (45 μm fineness: 13.2% retained), it was more difficult to maintain an adequate air void system and control the salt scaling resistance at later age (91 days). With coarser fly ash (45 μm fineness: 26.6% retained), salt scaling after 28 severe freeze/thaw cycles equaled only 0.5 kg/m^2. Nevertheless, AEA use increased the water sorption under vacuum and the apparent gas permeability.

1. Introduction

Although the concept of high-volume fly ash (HVFA) concrete has been proven successful in many, mostly less demanding concrete applications (e.g. foundations) [1], its use in more critical environments is still not common practice. Indeed, many concrete manufacturers remain skeptical about replacing the majority portion of the cement with pozzolanic fly ash from coal fired electrical power plants. In freeze/thaw environments with the presence of deicing salts, this is mainly because the performance of these concrete compositions is unsatisfactory when subjected to accelerated salt scaling tests in the laboratory. Malhotra and Mehta [1] have reported a higher deterioration rate for HVFA concrete under laboratory conditions cf. ASTM C672 [2]. However, the use of this concrete type in the field indicated otherwise. Concrete pavement in Wisconsin (US) and sidewalk sections in Halifax (Canada) made with HVFA concrete and subjected to deicing salts, exhibited a good performance [1]. Nevertheless, the applicable European standard NBN EN 1339 [3] does not specify a criterion for the concrete's behaviour under realistic conditions. Instead, a limiting value of 1 kg/m^2 is specified as the maximum mass loss per unit area after 28 severe freeze/thaw cycles with temperatures ranging from −18 to 20 °C in 24 h [3].

Also note that some differences exist between concrete standards regarding the required minimum air content in the fresh state to achieve an acceptable salt scaling resistance. According to the European standard NBN EN 206-1 [4], concrete exposed to freeze/thaw in combination with deicing salts should be air entrained and have an air content of at least 4% in the fresh state. However, according to the Belgian standard NBN B 15-001 [5] artificial air entrainment is not mandatory and if used, it should relate to the maximum aggregate size of the concrete. For a maximum nominal aggregate size of 16 mm, it specifies an air content of at least 5%. The American standard ACI 201.2R [6] also takes into account the higher air requirements of concrete mixtures with higher paste contents due to smaller nominal maximum aggregate sizes. However, also the severity of the exposure is of importance in this standard. A distinction is made between moderate and severe exposures. Exposure conditions are considered to be severe whenever deicing salts are present. In such an environment, an air content of 6–7% is recommended for a maximum nominal aggregate size of 16 mm. 5–5.5% Of air is only sufficient in the case of moderate exposure (without deicing salts) for the same aggregate size. Nevertheless, the recommendations of ACI 201.2R [6] are not binding. Local conditions and experience with specific mixtures and procedures could still warrant other values.

Within the scope of this paper, we have developed a HVFA mixture that should meet the salt scaling criterion of 1 kg/m^2 based on the chosen air content in its fresh state. In a first research phase, the air void system in the hardened state (air content, spacing factor, etc.) was characterized by means of microscopic analysis on thin sections and air void analysis conforming to ASTM C457 [7]. In a second research phase, the salt scaling resistance of the concrete's cast surface was tested according to the procedure de-

* Corresponding author. Tel.: +32 9 264 55 22; fax: +32 9 264 58 45.
E-mail address: nele.debelie@ugent.be (N. De Belie).

0958-9465/$ - see front matter © 2013 Elsevier Ltd. All rights reserved.
http://dx.doi.org/10.1016/j.cemconcomp.2013.01.005

scribed in NBN EN 1339 [3]. The effectiveness of the applied air entraining agent (AEA) in combination with fly ash was investigated for fly ashes from two different sources. In a third research phase, it was investigated whether the addition of an AEA can make steel reinforced HVFA concrete more susceptible to other important deterioration mechanisms that strongly depend on the permeability of the concrete, e.g. steel corrosion. In the literature, this impact has rarely been studied. Corrosion can be initiated by the chlorides from deicing salts entering the concrete or by concrete carbonation due to a constant exposure to exhaust fumes from motorized traffic. To evaluate the real impact of these mechanisms on the corrosion resistance, the material needs to be exposed to chlorides and CO_2 concentrations as present in the natural environment. Since this approach is usually quite time consuming, two influencing parameters (water penetrability and gas permeability) were studied instead of performing the required realistic chloride diffusion and carbonation tests. With respect to carbonation-induced corrosion, the accessibility to water and the permeability to air are very relevant parameters to be studied [8]. The same holds true for chloride-induced corrosion.

2. Materials and methods

2.1. Concrete mixtures

In total, six concrete mixtures were manufactured with the intention to be used in exposure class XF4 (cf. NBN EN 206-1 [4]): concrete exposed to significant attack by freeze/thaw cycles while wet, with high water saturation and deicing salts or sea water (Table 1). Two of these concrete compositions were considered as a reference concrete. Mixture T(0.45) is a non-air entrained ordinary Portland cement (OPC) concrete with the minimum cement content and the maximum water-to-cement ratio (W/C) conforming to the Belgian standard NBN B15-001 [5] for this type of environment. An air entrained version of the reference concrete mixture (T(0.45)A) conforming to NBN EN 206-1 [4] was also manufactured. The incorporation of a fatty acid/polyglycol based air entraining agent (dry matter mass percentage: 4%) is indicated within the concrete mixture name by means of the letter 'A'. Since the initial air content equaled 6.8%, this reference concrete should be a suitable concrete for exposure to severe conditions (cf. ACI 201.2R [6]). Since a traditional concrete for exposure class XF4 does not necessarily have to be air entrained according to NBN B15-001 [5], both non-air entrained HVFA mixtures (F(1)50 and F(2)50) and air entrained HVFA mixtures (F(1)50A and F(2)50A) were evaluated in this research. The mixing time for each mixture was 5 min: 1 min of dry mixing, 2 min of mixing after adding the mixing water and another 2 min of mixing after adding the polycarboxylic ether-based superplasticizer (SP) (dry matter mass percentage: 35%). In case of air entrainment, the AEA was added to the mixing water before being added to the binder, sand and aggregates. Each HVFA composition was made twice: once with fly ash F(1) and once with fly ash F(2). Both of them meet the requirements as specified in NBN EN 450-1 [9] to qualify for use in concrete: the loss on ignition (4.79% and 4.42%, respectively) was lower than 5% (Class A) and the 45 μm fineness was less than 40% (13.2% versus 26.6% retained, respectively). The difference in fineness is also confirmed by the clear difference in specific surface between F(1) and F(2) as obtained with the Blaine method and laser diffraction measurements (Table 2).

It should also be noted that all HVFA mixtures are characterized by a higher binder content B (cement + fly ash), a lower water-to-binder ratio (W/B), and a lower aggregate content compared to the references T(0.45) and T(0.45)A. This was mainly done to ensure a strength class equal or higher than the minimum (C30/37) required for an XF4 environment according to NBN EN 206-1 [4] and NBN B15-001 [5]. However, this approach resulted in a higher compressive strength for the HVFA mixtures F(1)50, F(1)50A and F(2)50.

2.2. Curing and sample pre-conditioning

Four $400 \times 400 \times 100\ mm^3$ concrete slabs and twelve cubes with a side length of 150 mm were cast per mixture. After casting, the specimens were kept at a constant temperature and relative humidity of 20 °C and 95%, respectively. Demoulding took place the next day whereupon the slabs and cubes were stored again under the same conditions until the age of testing. All tests were conducted after 28 and 91 days of curing to see whether the formation of additional hydration products due to the pozzolanic reaction of the fly ash can influence the air void system in the hardened state.

The specimens used for microscopic analysis on thin sections, air void analysis and measurement of the gas permeability were all taken from the slabs, while the cylinders for the vacuum saturation test were obtained from cubes. The capillary sorption test was performed on cubes.

The capillary water uptake, the permeable porosity and the gas permeability were measured after oven drying to constant mass (<0.1% mass change within 24 h) at 40 °C. Usually, this took about 14 days. Afterwards, the measurements were repeated on the same specimens after oven drying at 105 °C. The latter drying procedure removes all capillary and gel water from the concrete [10]. A predrying temperature of 105 °C was also proposed by Boel et al. to successfully measure concrete's gas permeability at a water satura-

Table 1
Mixture proportions, water-to-binder ratio (W/B), the applied dosage of air entraining agent (AEA) and superplasticizer (SP), the air content, the air-to-paste ratio, the slump and the compressive strength class of the tested concrete compositions.

	T(0.45)	T(0.45)A	F(1)50	F(1)50A(-2)	F(2)50	F(2)50A(-2)
Sand 0/4 (kg/m^3)	715	715	645	645	645	645
Aggregate 2/8 (kg/m^3)	515	515	465	465	465	465
Aggregate 8/16 (kg/m^3)	671	671	606	606	606	606
CEM I 52.5 N (kg/m^3)	340	340	225	225	225	225
Fly ash (kg/m^3)	–	–	225	225	225	225
Water (kg/m^3)	153	153	158	158	158	158
W/B	0.45	0.45	0.35	0.35	0.35	0.35
AEA (ml/kg B)	–	2.0	–	5.0 (7.0)	–	5.0 (7.0)
SP (ml/kg B)	2.0	4.0	7.0	7.0 (4.0)	5.0	5.0 (4.0)
Air content (%)	2.8	6.8	2.6	5.2 (6.9)	2.8	4.9 (7.3)
Air-to-paste (%)	10.6	25.0	7.9	15.6 (20.5)	8.5	14.7 (21.6)
Slump[a]	S2	S5	S5	S5 (S1)	S5	S5 (S2)
Strength class	C55/67	C35/45	C45/55	C40/50	C40/50	C30/37

[a] S1 (10–40 mm), S2 (50–90 mm), S3 (100–150 mm), S4 (160–210), S5 (⩾220 mm).

Table 2
Physical and chemical characteristics of the cement and fly ash types. The densities and specific surfaces (*) for the cement CEM I 52.5 N were provided by the cement manufacturer. The specific surfaces of the fly ashes were measured in two ways: once using the Blaine method and once with a laser diffractor.

	CEM I 52.5 N	F(1)	F(2)
LOI (%)	1.5	4.8	4.4
45 μm Fineness (%)	–	13.2	26.6
Density (kg/m^2)	3120*	2230	2260
Specific surface, Blaine method (m^2/kg)	390*	415	288
Specific surface, laser diffractor (m^2/kg)	–	366	262
CaO (%)	63.37	2.80	7.58
SiO_2 (%)	18.90	48.54	50.83
Al_2O_3 (%)	5.74	33.34	20.45
Fe_2O_3 (%)	4.32	3.52	7.52
SO_3 (%)	3.34	0.80	0.68
MgO (%)	0.89	0.72	1.77
Na_2O (%)	0.47	0.34	1.00
K_2O (%)	0.73	1.54	1.69

tion degree of 0% [11]. Drying at 105 °C is sometimes subject to criticism as the method may induce pore collapse and a modification of the stoichiometry and density of the calcium silicate hydrate gels (C–S–H) [12,13]. However, the same drying temperature has been successfully applied to measure the total porosity of concrete by means of hydrostatic weighing after vacuum saturation. This porosity seems to be only slightly higher in comparison with the one deduced from experimental water vapour desorption isotherms [14]. Compared to total porosities calculated from phase assemblage of the present hydrates, the measured porosities through hydrostatic weighing and oven drying at 110 °C are also only slightly higher [15]. Nevertheless, it needs to be noted that in addition to total porosity, pore connectivity and size are also important for the transport properties of concrete. Despite the successful use of the higher drying temperature according to the literature, it was decided to first measure the capillary water uptake, the permeable porosity and the gas permeability after pre-drying at a lower temperature (40 °C), before measuring the same parameters after pre-drying at 105 °C.

In the results section, all figures present the mean values and error bars indicate the standard deviation on the individual values.

2.3. Microscopic analysis on thin sections

45 × 30 × 15 mm^3 Prisms (n = 3) were sawn in such a way that a 45 × 15 mm^2 face was a cast surface. First, one 45 × 30 mm^2 face was glued onto a glass slide with a thickness of 2.9 mm. Then, the samples were cut and polished until the height of the concrete specimens and the glass equaled 10.1 mm. In a next step, the samples were impregnated under vacuum with a fluorescent epoxy. After impregnation, the excess epoxy was ground away and an object glass was glued onto the polished surface. In a final step, the glass slides were cut off and the concrete samples on the object glasses were polished until thin sections with a 25 μm thickness were obtained. A cover glass was glued onto them for protection. All thin sections were examined with a Leica DM LP polarizing microscope. A magnification of 50× was used. The luminous intensity of the polarized light equaled 5 on a scale of 10. The microscopic analysis on thin sections enabled a qualitative study of the air void system. Per concrete mixture and curing period, a series of photos was taken of the thin sections as observed under the microscope. Per thin section, 3 photos were taken near the cast surface and 3 photos near the saw cut surface. This resulted in 6 photos per thin section and thus 18 photos per concrete mixture at each age. Since visual observation showed no obvious differences between them, only one representative photo of each concrete mixture was included in Fig. 1.

2.4. Air void analysis

A more quantitative air void analysis is possible with the RapidAir 457 apparatus. In accordance with ASTM C457 [7], the linear traverse method was used to determine the air content and air void distribution of the hardened concrete. The test was performed on cylindrical specimens (n = 4, Diameter (D) = 80 mm, Height (H) = 20 mm). The technique required a careful polishing of the sample surfaces since scratches are to be avoided and air voids must have sharp edges [16]. Therefore, the following polishing procedure was used. First, the sample surfaces were mechanically flattened. Then, the surfaces were subsequently treated with eight different wet diamond polishing pads (grit 50, 100, 200, 400, 800, 1500, 3000 and 8000). Before using each polishing pad, a raster was drawn onto the surfaces with chalk. Each time, the polishing with one pad continued until the chalk raster had completely disappeared from the surface.

Contrast enhancement was realized as follows: the polished surfaces were coloured with black ink and white $BaSO_4$ powder (maximum particle size ⩽2 μm) was distributed on top to fill the air voids. After removing the excess powder with a steel blade, the specimens were ready for testing. The threshold value for analysis equaled 221 on a 0–256 scale. All samples were analyzed in two perpendicular directions using 10 probe lines per frame with a total traverse length of 17,733 mm and a scanned area of 50 × 50 mm. With the recorded total chord length of air voids T_a (mm) and paste T_p (mm), the total surface distance traversed across T_{tot} (mm), the total number of air void chord lengths N (−) and the paste content p (%) for each concrete composition, the concrete's air void system can be fully characterized. Air contents A (%), specific surfaces α (mm^{-1}), spacing factors L_S according to Powers (μm) and average chord lengths l_m (mm) were calculated using the following equations:

$$A = \frac{T_a}{T_{tot}} \times 100 \tag{1}$$

$$\alpha = \frac{4N}{T_a} \tag{2}$$

$$L_S = \frac{T_p}{4N} \quad (\text{for } p/A \leqslant 4.33) \text{ or } L_S = \frac{3}{\alpha}\left[1.4\left(1+\frac{p}{A}\right)^{1/3} - 1\right] \quad (\text{for } p/A > 4.33) \tag{3}$$

$$l_m = \frac{T_a}{N} \tag{4}$$

2.5. Deicing salt scaling resistance

Deicing salt scaling resistance was evaluated in accordance with NBN EN 1339 [3]. Cylinders (n = 6, D = 100 mm, H = 50 mm) were glued into a piece of insulated PVC tube with the casting surface upwards. A 5 mm thick water layer was put on top of the cylindrical test surfaces for at least 72 h to check for leakages. Next, the water layer was replaced with a 5 mm thick 3% NaCl solution after which the specimens were subjected to 28 severe freeze/thaw cycles in a freezing chamber where temperatures ranged from −18 to 20 °C in 24 h. Every 7 days, the scaled off material was collected, dried at 105 °C and weighed in order to determine the mass loss per unit area (Δm).

2.6. Time dependent monitoring of the air content

Besides the measurement of the initial air content (Table 1), a time dependent monitoring of the air content was also considered

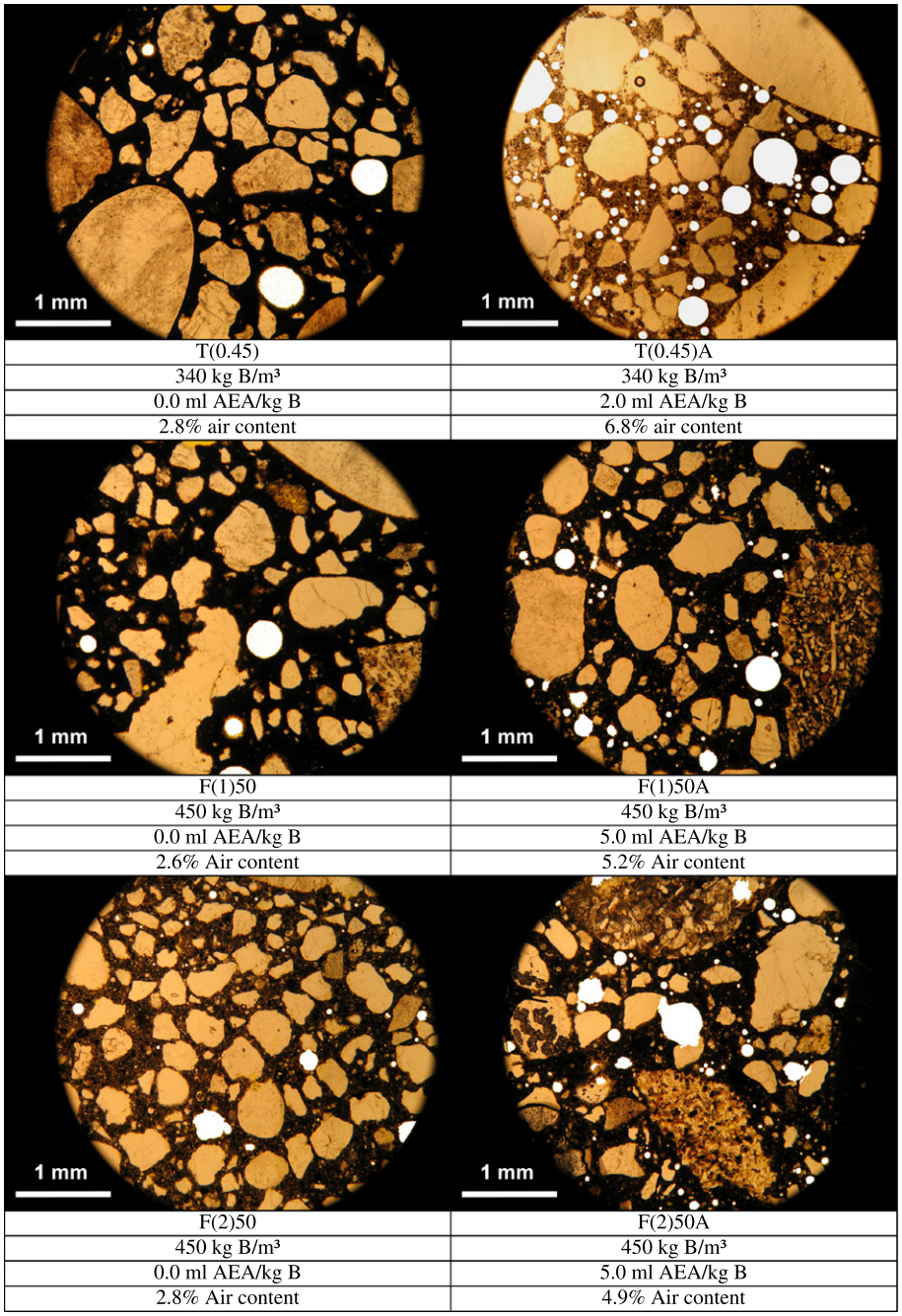

Fig. 1. Microscopic analysis of the air void system (coloured white) clearly shows the effect of applying an AEA (A), though a somewhat less pronounced air void system seems to be present in F(1)50A. The microscopic images in colour are available online.

on small batches (40 l) of each air entrained concrete mixture using the same SP dosage of 4.0 ml/kg B (Table 4). This was the dosage needed to achieve the highest slump class for at least one of the mixtures that was studied on small scale (a 40 l batch). This dosage was then used for all the other mixtures as well.

The applied test procedure was similar to the one followed by Zhang [17]: 15 min after mixing, the air content was determined with a TESTING Air entrainment meter (capacity: 8 l). The remaining concrete was then mixed for 5 min and allowed to stand for 5 min. This procedure was repeated twice whereafter the air content and slump were measured again 60 min after the initial mixing. In addition, Zhang's experimental procedure was extended with the measurement of the air content after 120 min.

2.7. Water penetrability

The amount of water penetrating the concrete differs with the prevailing transport mechanism, the saturation degree and the exposure time of the material. Analogous to previous work by the authors, two scenarios were evaluated experimentally and compared with each other [18].

2.7.1. Capillary water sorption

When a non-saturated concrete element is in contact with water at one side and evaporation is possible from the other side, the water can be capillary absorbed [10]. As poor water drainage is sometimes a problem around buildings and structures, the moti-

vation for evaluating this phenomenon is clear. The capillary sorption behaviour of the investigated concrete mixtures was evaluated using a test method similar to the one described in the Belgian Standard NBN B15-217 [19]. Note that the 40 °C drying temperature is only slightly different from the drying temperature (50 °C) prescribed in ASTM C 1585-04e [20] to measure capillary sorption. After weighing the oven dried cubes ($n = 3$, $H = 150$ mm), they were put on rods in a water bath in such a way that they were immersed for 5 mm. To obtain unidirectional flow, the sides adjacent to the inflow face were covered with a self-adhesive aluminium tape. The experiment was carried out in a climate chamber with a constant temperature of 20 ± 2 °C and a relative humidity of 60 ± 5%. For each specimen and pre-drying temperature, the mass increase after 14 days was measured and the corresponding capillary water uptake per unit area was calculated.

2.7.2. Water sorption under vacuum

In laboratories, concrete's accessibility to water can be evaluated in different ways. For instance, it is possible to measure the amount of water absorbed under vacuum. Vacuum saturation tests were performed for all six compositions on cylindrical concrete specimens ($n = 9$, $D = 100$ mm, $H = 50$ mm). After measuring the oven dry masses ($m_{d\ 40°C/105°C}$), the samples were put in a tank where a vacuum with a residual pressure of 2.7 kPa was created for 2.5 h. Then, water was introduced at a rate of 50 mm/h until complete submersion of the samples. Subsequently, air pressure was restored and the samples were kept under water for 24 h. A similar vacuum saturation technique is mentioned in ASTM C 1202-05 [21]. The procedure described here is in accordance with the Belgian Standard NBN B05-201 [22] and allows the calculation of a permeable porosity φ (%) using the following equation:

$$\varphi = 100 \cdot \frac{m_{s\ 40°C/105°C} - m_{d\ 40°C/105°C}}{m_{s\ 40°C/105°C} - m_{l\ 40°C/105°C}} \quad (5)$$

Within this formula, $m_{l\ 40°C/105°C}$ and $m_{s\ 40°C/105°C}$ stand for the mass under water and the water saturated mass after vacuum saturation, respectively. Drying at 105 °C is in correspondence with the drying procedure described in ASTM C 642-06 [23]. In the literature, similar hydrostatic weighing techniques have been used successfully to measure porosity [14,15]. All methods required oven drying at an elevated temperature ranging from 105 °C to 110 °C and were published in test method recommendations [24] and national standards [22,25].

2.8. Gas permeability

After pre-drying, the O_2 flow rate Q (ml/s) and the corresponding apparent oxygen permeability k_a at 2 bar pressure were measured on cylindrical specimens ($n = 3$, $D = 150$ mm, $H = 50$ mm) using the 'cembureau' permeameter mentioned in RILEM TC 116-PCD [26].

Before each measurement, a certain waiting period (±half hour) was required to obtain a steady gas flow rate Q (ml/s) through the three cylindrical specimens. The apparent oxygen permeability k_a of each mixture was calculated by means of Eq. (6) [27], without performing a Klinkenberg correction [28].

$$k_a = \frac{2Q}{A} \frac{\mu LP}{(P^2 - P_a^2)} \quad (6)$$

The other parameters in Eq. (2) are: the cross-sectional area A of the specimen (m^2), the thickness L of the specimen (m), the dynamic viscosity μ of the fluid (2.02×10^{-5} N s m^{-2} for O_2 at 20 °C), the atmospheric pressure P_a (bar) and the absolute inlet pressure P (2 bar).

3. Results and discussion

3.1. AEA dosage and air content in the fresh state

The incorporation of fly ash in concrete has an impact on the required AEA dosage (Table 1). For the reference T(0.45)A, a dosage of 2.0 ml/kg binder was sufficient to have an air content (6.8%) conforming to all standards. This air content was recorded 15 min after mixing with a TESTING Air entrainment meter (capacity: 8 l). With respect to the air entrained HVFA mixtures F(1)50A and F(2)50A, a much higher AEA dosage (5.0 ml/kg binder) resulted in an air content that was considerably lower than the 6.8% of the reference: 4.9% for mixture F(1)50A and 5.2% for mixture F(2)50A. As a consequence, the air content criterion imposed by ACI 201.2R [6] was not met.

Also note that besides the air content (which is the air-to-concrete ratio), the air-to-paste (A/P) ratio is often used to evaluate the concrete's air void system. This is mainly done because it is the paste and not the aggregate fraction that requires air entrainment. An air void system having a total volume of about 18–20% of the paste volume should protect the paste against freeze/thaw damage [29,30]. As can be seen from Table 1, the air-to-paste ratio of mixture T(0.45)A exceeds the recommended 18–20% range (A/P: 25.0%), while F(1)50A and F(2)50A have air-to-paste ratios below the optimal range (15.6% and 14.7%, respectively). The optimal initial air content corresponding with the recommended air-to-paste range was calculated for each air entrained concrete mixture. For mixture T(0.45)A an air content of 4.8–5.3% would be enough, while for F(1)50A and F(2)50A, the air contents should equal 6.0–6.7% and 6.0–6.6%, respectively, as the HVFA concretes have a considerably lower total aggregate volume fraction. However, this was not the case for the air entrained HVFA mixtures that were studied initially.

Therefore, two additional air entrained HVFA mixtures with an increased AEA dosage (7.0 ml/kg B instead of 5.0 ml/kg B) were made: F(1)50A-2 and F(2)50A-2. Their estimated air-to-paste ratios (F(1)50A-2: 20.5%, F(2)50A-2: 21.6%) were calculated from the fresh air contents measured 15 min after mixing (Table 4: F(1)50A-2: 6.9%, F(2)50A-2: 7.3%) and found to be more or less in agreement with the suggested 18–20% criterion. Its effect on the hardened air void system and the salt scaling resistance after 28 and 91 days, was also assessed experimentally by means of automated air void analysis (Section 3.3) and the accelerated freeze/thaw test (Section 3.4).

3.2. Thin sections

A comparison between the different mixtures with air entrainment, indicates that the use of a rather high dosage of AEA (5.0 ml/kg B, Table 1) did not result in a very pronounced system of artificial air bubbles inside the concrete matrix for mixture F(1)50A (Fig. 1). On the other hand, the incorporation of the same dosage of AEA in mixture F(2)50A did result in an air void system similar to the reference T(0.45)A. However, with respect to the latter mixture this was achieved by means of a much smaller AEA dosage (2.0 ml/kg B, Table 1). This difference between the mixtures F(1)50A and F(2)50A is not in agreement with the similar air contents which were measured in fresh state (5.2% versus 4.9%, Table 1). For all non-air entrained concretes, few air bubbles could be observed.

However, a correct characterization of the concrete's air void system cannot be done by just looking at thin sections. Conclusions drawn from these merely visual observations are qualitative and should be supported by a quantitative study of all relevant param-

eters with respect to this air void system. This was done with automated air void analysis.

3.3. Air void analysis

The total air content is the parameter usually specified since it is easily measurable in the field [6]. Although the minimum air contents mentioned in Section 2.1 normally apply to the air content in the fresh state, the values obtained for the hardened concrete were evaluated according to the same criteria (Fig. 2a). Compared to T(0.45), the air entrained reference T(0.45)A was characterized by a much higher air content (7.5–8.0%). Note that the higher values for the T(0.45)A reference mixture are somewhat different from its initial air content (6.8%, Table 1) in the fresh state. Moreover, it was observed that in addition to the presence of the smaller regular shaped air voids due to air entrainment, all sample surfaces of T(0.45)A contained some larger – more than 1 mm in cross-section – irregular shaped air voids, likely entrapped as opposed to entrained air. There may be two possible explanations for the difference between the air content in fresh and hardened state. Either the entrapped air has evolved after the initial air content measurements, or it was removed more effectively from the fresh concrete that was used for the air content measurements than from the concrete used to cast the concrete specimens (Section 2.2).

According to St. John et al. [31] the maximum diameter of an entrained air void is 1 mm. This criterion could be used to separate the entrained from the entrapped air. Now, the air void analysis technique enables the determination of an air content based on all chord lengths traversed during the analysis and an air content solely based on the traversed chord lengths <1 mm. Although looking at the latter air content will obviously result in an overestimation of the actual entrained air content (it considers all traversed chord lengths of the voids and not just the diameters), it provides a first rough estimation of the entrained–entrapped air proportions. The total air content of the non-air entrained reference T(0.45) was found to consist of 52–55% for air voids with chord lengths <1 mm. For T(0.45)A this value increased to 92–93% (Table 3). Thus, despite the presence of some larger entrapped air voids, the artificial entrainment of air voids was quite effective after all. It also means that an explanation for the difference between the air contents in fresh and hardened state must be sought elsewhere (Section 3.7.1).

Regarding the HVFA compositions, air entrainment resulted in an increase of the air content, though the values obtained were lower than 6–7%. Compared to F(1)50 and F(2)50, the average hardened air contents of F(1)50A and F(2)50A were increased by only 1.8% and 1.5%, respectively. The air contents in hardened state were more or less in accordance with the measured air contents in the fresh state (F(1)50A: 4.9%, F(2)50A: 5.2%). When looking at the ratio between the air contents calculated from the traversed chords <1 mm and those calculated from all chords traversed, the following conclusions can be drawn. With the use of fly ash F(1), adding 5.0 ml AEA/kg binder to the concrete resulted in an increase of this ratio from 62–63% to only 74–75%. With the use of fly ash F(2) and the same AEA dosage, this ratio increased from 55–58% to 73–78%. Thus, in contrast with the 92–93% air content ratio of mixture T(0.45)A, the corresponding values of the two air entrained HVFA mixtures are considerably lower. From both the differences in total air content and entrained–entrapped air content proportioning, it can already be observed that the artificial air entrainment of mixtures F(1)50A and F(2)50A was less successful despite an AEA dosage of 5.0 ml/kg B.

Not only a sufficient total air content is of importance, but also an adequate distribution of the artificial air bubbles. In other words, their spacing should be close enough to prevent the development of pressures from freezing which would fracture the concrete. The fulfillment of this requirement is usually evaluated through the calculation of a spacing factor L_S for the concrete. This is the maximum distance from any point within the concrete matrix to the edge of the nearest air bubble. A L_S of 200 μm is recommended as the maximum for concrete exposed to freeze/thaw attack [5,6]. The spacing factors of all air entrained concrete compositions (T(0.45)A, F(1)50A, F(2)50A) do not exceed this maximum value after both 28 and 91 days of curing, although the HVFA mixtures are characterized by somewhat higher values (Fig. 2b: 100–200 μm) when compared with the OPC reference (Fig. 2b: ±100 μm). Without air entrainment, the spacing factors of T(0.45), F(1)50 and F(2)50 range between 250 and 350 μm.

Besides the spacing factor L_S, the specific surface α also characterizes the distribution of the air bubbles (Fig. 2c). The higher the value for α, the more the air void system consists of finer pores which contribute to the salt scaling resistance. For air entrained concrete designed in accordance with ACI 201.2R the specific surface α is usually in the range 25–45 mm^{-1} [6]. All air entrained concrete mixtures (T(0.45)A, F(1)50A and F(2)50A) exhibited a

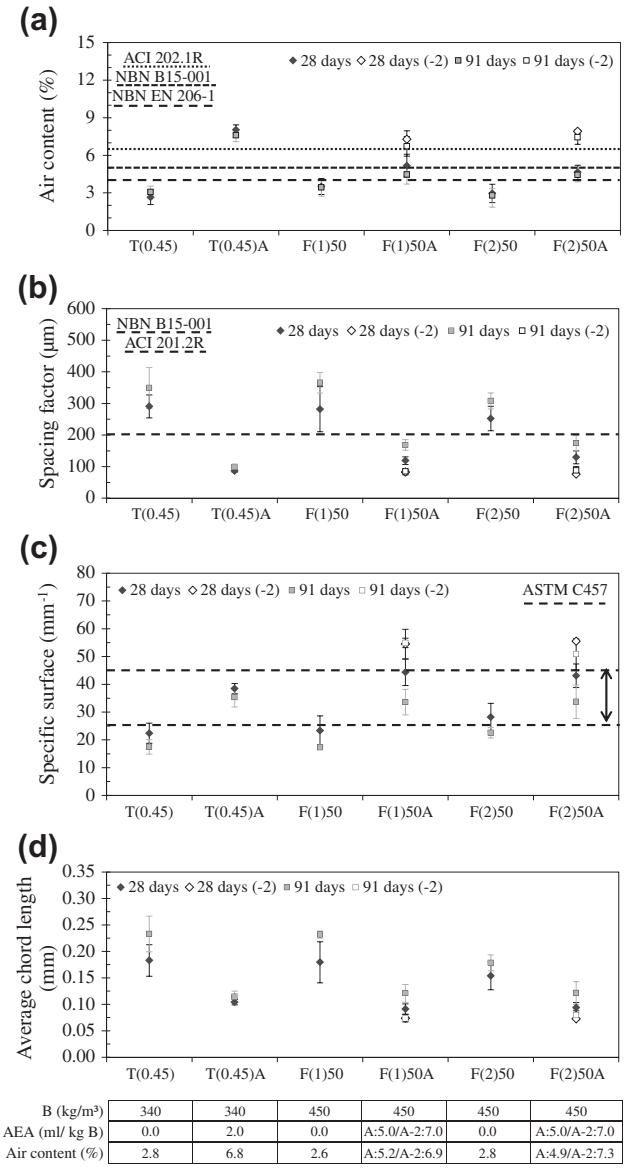

	T(0.45)	T(0.45)A	F(1)50	F(1)50A	F(2)50	F(2)50A
B (kg/m³)	340	340	450	450	450	450
AEA (ml/ kg B)	0.0	2.0	0.0	A:5.0/A-2:7.0	0.0	A:5.0/A-2:7.0
Air content (%)	2.8	6.8	2.6	A:5.2/A-2:6.9	2.8	A:4.9/A-2:7.3

Fig. 2. Influence of AEA use on the air content (a), the spacing factor (b), the specific surface (c) and the average chord length (d) of the reference and the HVFA mixtures as obtained from automated air void analysis after 28 and 91 days of curing.

Table 3
Difference between the air contents calculated from all traversed chords and the air contents calculated from the traversed chords <1 mm during an automated air void analysis.

A (%)	T(0.45)	T(0.45)A	F(1)50	F(1)50A	F(2)50	F(2)50A
28 days						
All chords	2.7 ± 0.6	8.0 ± 0.4	3.5 ± 0.6	5.2 ± 0.9	3.0 ± 0.7	4.6 ± 0.6
Chords <1 mm	1.4 ± 0.2	7.5 ± 0.5	2.2 ± 0.5	3.8 ± 0.6	1.7 ± 0.3	3.6 ± 0.5
Ratio (%)	52	93	63	73	57	78
91 days						
All chords	3.1 ± 0.5	7.6 ± 0.5	3.4 ± 0.6	4.5 ± 0.8	3.1 ± 0.9	4.4 ± 0.5
Chords <1 mm	1.7 ± 0.3	7.0 ± 0.4	2.2 ± 0.5	3.3 ± 0.1	1.8 ± 0.3	3.2 ± 0.2
Ratio (%)	55	92	65	73	58	73
				F(1)50A-2		F(2)50A-2
28 days						
All chords				7.2 ± 0.7		7.9 ± 0.2
Chords <1 mm				6.1 ± 0.6		7.2 ± 0.1
Ratio (%)				85		91
91 days						
All chords				6.7 ± 0.8		7.4 ± 0.6
Chords <1 mm				6.2 ± 0.4		6.8 ± 0.8
Ratio (%)				93		92

Table 4
Influence of the binder type on the evolution of the air content with time, as measured after 15, 60 and 120 min, for the applied AEA and SP dosages. When comparing the two HVFA mixtures, note that it is easier to obtain and maintain a high air content (6–7%) in mixture F(2)50A(-2).

Time (min)	Parameter	T(0.45)A 2.0 ml AEA/kg B 4.0 ml SP/kg B	F(1)50A 5.0 ml AEA/kg B 4.0 ml SP/kg B	F(2)50A 5.0 ml AEA/kg B 4.0 ml SP/kg B
15	Slump[a]	S5	S2	S5
	Air content	6.8%	4.6%	4.0%
60	Slump[a]	S3	S1	S1
	Air content	9.5%	3.8%	7.2%
120	Slump[a]	S1	S1	S1
	Air content	7.8%	4.0%	6.6%
			F(1)50A-2 7.0 ml AEA/kg B 4.0 ml SP/kg B	F(2)50A-2 7.0 ml AEA/kg B 4.0 ml SP/kg B
15	Slump[a]		S1	S2
	Air content		6.9%	7.3%
60	Slump[a]		S1	S1
	Air content		5.1%	7.7%
120	Slump[a]		S1	S1
	Air content		4.4%	7.7%

[a] S1 (10–40 mm), S2 (50–90 mm), S3 (100–150 mm), S4 (160–210), S5 (⩾220 mm).

higher specific surface than the non-air entrained compositions (T(0.45), F(1)50 and F(2)50). Since a higher value for the specific surface indicates the presence of finer pores, the air entrained concrete mixtures should have average chord lengths that are considerably lower than the ones recorded for the non-air entrained compositions. This was indeed the case (Fig. 2d).

Increasing the AEA dosage from 5.0 ml/kg B to 7.0 ml/kg B, resulted in a more adequate air void system in hardened state for HVFA concrete. The total air contents measured for F(1)50A-2 and F(2)50A-2 (Fig. 2a) slightly exceeded the 6–7% criterion recommended by the ACI 201.2R guideline [6]. 85–93% of the total air content consisted of the air content calculated from traversed chord lengths <1 mm (Table 3). Spacing factors decreased to values around 100 μm cf. T(0.45)A (Fig. 2b). The compositions were characterized by the highest specific surfaces (Fig. 2c: ±55 mm^{-1}) and the lowest average chord lengths (Fig. 2d: ±0.075 mm).

In conclusion, compared to T(0.45)A, the air entrained HVFA mixtures F(1)50A and F(2)50A are characterized by a lower air content and a somewhat higher, yet still acceptable spacing factor. As a consequence, the mixtures with fly ash may be more susceptible to salt scaling. On the other hand, specific surface and average chord length recordings indicate that the air void systems of F(1)50A and F(2)50A contain more small air bubbles which may improve the resistance to salt scaling. Note that with a high value for the specific surface α, a suitable spacing factor L_S can still be obtained even when the air content is lower. However, in order to obtain an air void system that has both the volume capacity and the geometric parameters necessary to protect saturated mature cement paste during exposure to freezing, it is important to obtain concrete with an acceptably high air content and a low enough spacing factor [32]. To obtain this sufficiently high air content a further increase of the AEA dosage (from 5.0 ml/kg B to 7.0 ml/kg B) for the studied HVFA compositions was imperative. This intervention turned out to be beneficial for the four parameters characterizing the hardened air void system (air content A, spacing factor L_S, specific surface α and average chord length l_m). The actual impact of these properties on the salt scaling resistance has been investigated in Section 3.4.

3.4. Salt scaling resistance

From Fig. 3 it is clear that ordinary Portland cement concrete does not necessarily require air entrainment to ensure limited salt scaling. After 28 days of curing, the total amount of scaled off material at the end of the test is lower than 1 kg/m^2. After 91 days, the mean mass loss per unit area Δm is only slightly higher than the maximum value. The acceptable mass loss per unit area for T(0.45) supports the choice of this concrete composition as a reference concrete type for an XF4 environment in NBN B 15-001 [5]. Secondly, the addition of a limited amount of AEA (2.0 ml/kg B) to the same OPC concrete mixture was found to be very effective, since Δm was negligible after both 28 and 91 days of curing.

In contrast with reference mixture T(0.45), the performance of the non-air entrained HVFA mixtures subjected to the same experiment was far from acceptable. On average, Δm was more than twice the maximum mass loss allowed. Again, using an AEA significantly improved the salt scaling resistance. However, the effectiveness of the admixture was less than in reference T(0.45)A. Although the AEA dosage was more than doubled (5.0 ml/kg B versus 2.0 ml/kg B), higher mass losses per unit area were recorded for the HVFA mixtures F(1)50A and F(2)50A. The mean Δm value of HVFA mixture F(1)50A slightly exceeds the 1 kg/m^2 criterion at ages of 28 and 91 days. On the other hand, HVFA mixture F(2)50A performed very well after 28 days since the mass loss per unit area is only 0.4 kg/m^2. After 91 days, this amount in-

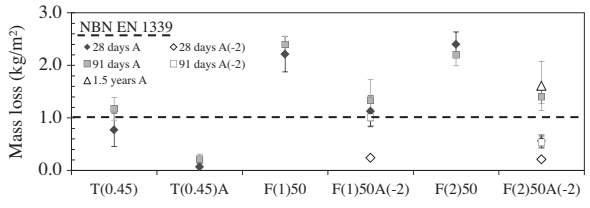

B (kg/m³)	340	340	450	450	450	450
AEA (ml/ kg B)	0.0	2.0	0.0	A:5.0/A-2:7.0	0.0	A:5.0/A-2:7.0
Air content (%)	2.8	6.8	2.6	A:5.2/A-2:6.9	2.8	A:4.9/A-2:7.3

Fig. 3. The use of an AEA clearly results in a significant decrease in mass loss due to salt scaling, though this decrease is significantly less for HVFA concrete ($n = 6$).

creased significantly to 1.4 kg/m^2. For all tested air entrained concrete mixtures, a small reduction in salt scaling resistance was observed between 28 and 91 days. Statistical analysis (Independent Sample *T* test, Significance level = 0.05) showed that only for mixture F(2)50A this difference was significant.

A reduction of the concrete's surface strength due to carbonation can be an explanation for the less than satisfactory salt scaling resistance after 91 days. This negative effect has already been reported for concrete containing blast-furnace slag [33]. Since HVFA concrete is also quite susceptible to the carbonation phenomenon, the same explanation could be valid. Now, possible carbonation of the concrete surface was not evaluated just before the salt scaling tests after 28 and 91 days of curing. This was done only afterwards for the air entrained HVFA mixtures. 10 mm thick slices were cut from 3 cubic F(2)50A concrete specimens (side length: 100 mm), and this after being stored in the curing room at 20 °C and 95% relative humidity for more than 1.5 years. Phenolphthalein was sprayed onto the slices to visualize and measure the carbonation front. The average carbonation depth equaled 2.0 ± 0.3 mm. The outcome of an additional salt scaling experiment done on the same concrete again showed that the amount of salt scaling ($\Delta m = 1.6 \pm 0.5$ kg/m^2) exceeded the 1 kg/m^2. However, this does not necessarily mean that carbonation is the sole cause for increased salt scaling of this concrete. It must be said that its air content in the hardened state was below the required minimum of 6–7%, as prescribed by ACI 201.2R [6]. Logically, it is difficult to assess the effect of carbonation on the salt scaling resistance of a concrete with an inadequate air void system. Therefore, we chose to do this evaluation only for HVFA mixtures F(1)50A-2 and F(2)50A-2 with the increased AEA dosage.

An adequate salt scaling resistance was confirmed for mixtures F(1)50A-2 and F(2)50A-2 with the higher air-to-paste ratios. For both of them, salt scaling remained far below the 1 kg/m^2 criterion after 28 days (F(1)50A-2: $\Delta m = 0.2 \pm 0.01$ kg/m^2, F(2)50A-2: $\Delta m = 0.2 \pm 0.03$ kg/m^2). The same goes for mixture F(2)50A-2 after 91 days ($\Delta m = 0.5 \pm 0.1$ kg/m^2. The salt scaling resistance of mixture F(1)50A-2 after 91 days is also still acceptable, although the mass loss increased to 1.0 ± 0.2 kg/m^2 (Fig. 3). The carbonation front prior to the salt scaling test was assessed on a dummy specimen of each concrete mixture after 28 and 91 days. The measured carbonation depths were found to be rather limited (max 1.0 mm) and no significant difference could be observed between the different mixtures and curing ages. Since limited carbonation was already observed for the specimens with very little salt scaling after 28 days (Δm: 0.2 kg/m^2), surface weakening due to carbonation cannot be seen as the main cause for increased scaling at later age.

3.5. Water penetrability

3.5.1. Capillary water sorption

As can be seen from Fig. 4, there is no significant difference in capillary water uptake w between the non-air entrained and the air entrained concrete mixtures after pre-drying at 40 °C. The w values of the HVFA mixtures were found to be slightly higher than the ones recorded for T(0.45) and T(0.45)A. Also after oven drying at 105 °C, no pronounced difference between the non-air entrained and the air entrained concrete mixtures could be observed. After 91 days of curing, mixture T(0.45)A absorbed significantly more water than mixture T(0.45). However, after pre-drying at 105 °C the *w* values of the former composition have a rather high standard deviation and should be interpreted with caution.

Note that increasing the pre-drying temperature to 105 °C somewhat changed the ranking in capillary water uptake between the OPC concrete and the HVFA concrete made with fly ashes F(1) and F(2). However, it did not result in an important difference between the non-air entrained and the air entrained variant of each concrete type.

3.5.2. Water sorption under vacuum

Addition of AEA always resulted in higher permeable porosities φ (%) for the OPC mixture and the HVFA mixture made with fly ash F(2). This effect could not be observed for the composition containing fly ash F(1) (Fig. 5).

After 28 days of curing, the porosities of the non-air entrained HVFA mixtures are significantly higher than the ones measured for T(0.45), and this for both drying temperatures (Fig. 5a). The fly ash type used did not seem to have an important impact. At the age of 91 days, the differences in porosity with T(0.45) were reduced (Fig. 5b).

3.6. Gas permeability

The addition of AEA resulted in higher gas permeabilities for all mixtures. At the age of 28 days, all air entrained concrete mixtures are clearly more permeable to gases than their non-air entrained equivalents (Fig. 6a). After pre-drying at 40 °C, the k_a value of T(0.45)A is at least two times the value of T(0.45). The same conclusion can be drawn when F(2)50 and F(2)50A are compared with

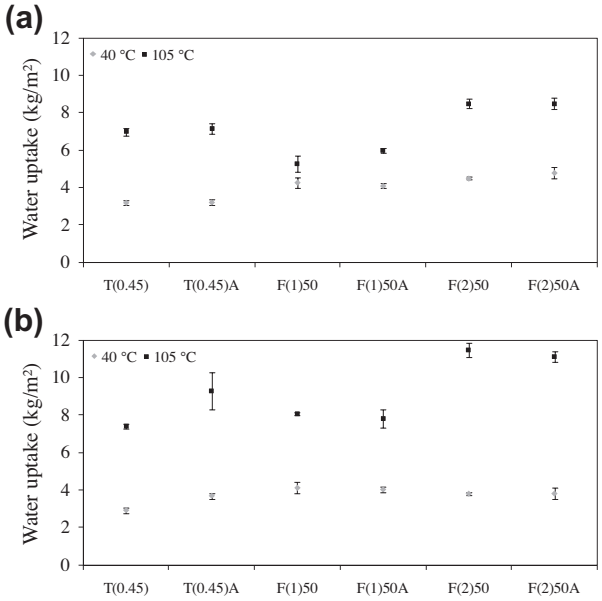

B (kg/m³)	340	340	450	450	450	450
AEA (ml/ kg B)	0.0	2.0	0.0	5.0	0.0	5.0
Air content (%)	2.8	6.8	2.6	5.2	2.8	4.9

Fig. 4. Influence of the concrete type (OPC or HVFA), the fly ash type (F(1) or F(2)) and the presence of AEA on the 14 days capillary water uptake *w* (kg/m^2) after 28 days (a) and 91 days (b) of curing ($n = 3$).

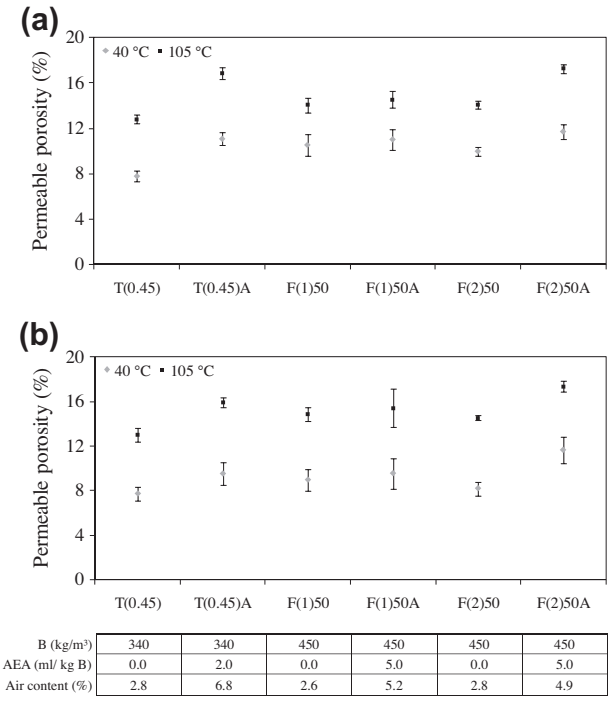

	T(0.45)	T(0.45)A	F(1)50	F(1)50A	F(2)50	F(2)50A
B (kg/m³)	340	340	450	450	450	450
AEA (ml/ kg B)	0.0	2.0	0.0	5.0	0.0	5.0
Air content (%)	2.8	6.8	2.6	5.2	2.8	4.9

Fig. 5. Influence of the concrete type (OPC or HVFA), the fly ash type (F(1) or F(2)) and the presence of AEA on the permeable porosity φ (%) after pre-drying at 40 °C and 105 °C and 28 days (a) and 91 days (b) of curing (n = 9). Note that no significant difference was recorded between the porosities of F(1)50 and F(1)50A.

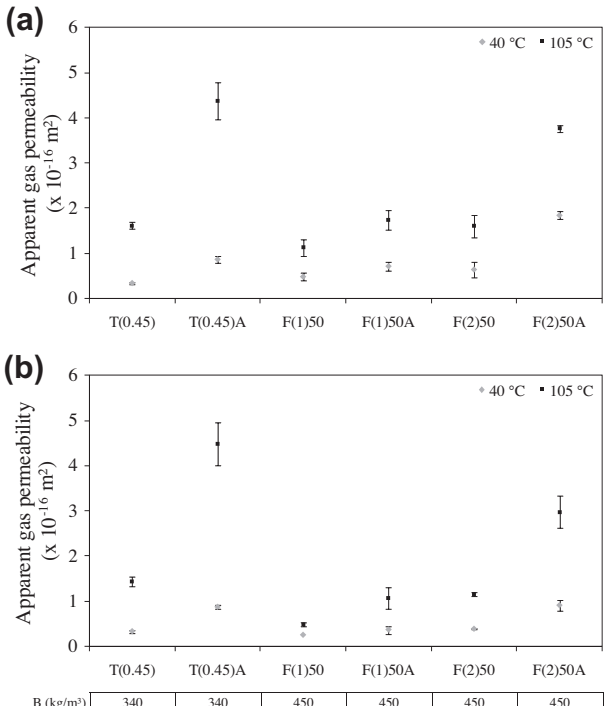

	T(0.45)	T(0.45)A	F(1)50	F(1)50A	F(2)50	F(2)50A
B (kg/m³)	340	340	450	450	450	450
AEA (ml/ kg B)	0.0	2.0	0.0	5.0	0.0	5.0
Air content (%)	2.8	6.8	2.6	5.2	2.8	4.9

Fig. 6. Influence of the concrete type (OPC or HVFA), the fly ash type (F(1) or F(2)) and the presence of AEA on the apparent gas permeability k_a ($\times 10^{-16}$ m^2) after 28 days (a) and 91 days (b) of curing (n = 3). Note that the differences are very pronounced after pre-drying at 105 °C and that the differences between F(1)50 and F(1)50A are small, especially after pre-drying at 40 °C.

each other. A much smaller difference exists between F(1)50 and F(1)50A. Pre-drying at 105 °C makes the differences between the non-air entrained and the air entrained concrete mixtures much more pronounced. Yet again, the smallest increase in apparent gas permeability was observed between F(1)50 and F(1)50A. After 91 days of curing, the findings can be considered as similar (Fig. 6b). Note that the k_a values of all HVFA mixtures decreased with prolonged curing.

3.7. General discussion

3.7.1. Relation: AEA dosage, achieved air void system and salt scaling resistance

The overall results indicate that it is possible to design a HVFA composition with an adequate salt scaling resistance under laboratory conditions. To achieve this, a lot of attention must be paid to the applied AEA dosage and the resulting air void system. Although the fresh air contents of the air entrained HVFA mixtures F(1)50A and F(2)50A were similar (5.2% and 4.9%, respectively), the air void system in the hardened state was different. Although the automated air void analysis did not reveal important differences between the two mixtures, microscopic analysis on thin sections clearly showed a much less pronounced air void system for mixture F(1)50A. Apparently, the initially entrained air content could not be maintained everywhere in the concrete until setting. Time dependent monitoring of the air content in the first hours after mixing resulted in the following findings (Table 4):

(i) With an AEA dosage of 5.0 ml/kg B, the air contents of mixture F(2)50A after 15 min, 60 min and 120 min amounted to 4.0%, 7.2% and 6.6%, respectively. Thus, intermittent mixing (to simulate handling on site) resulted in an important increase of the fresh air content after 60 min. By the time of the measurement after 120 min, the air content had only gradually decreased again. A similar behaviour was observed during the time dependent air content monitoring of OPC reference T(0.45)A. Mixture F(1)50A on the other hand was characterized by a slight decrease of the air content with time (15 min: 4.6%; 60 min: 3.8%; 120 min: 4.0%).

(ii) The clearly different evolution in air content was also detected during the time dependent air content monitoring of the HVFA mixtures with the higher AEA dosage (7.0 ml/kg B). A slight increase in air content was recorded for mixture F(2)50A-2, while the air content of mixture F(1)50A-2 decreases as a function of time.

All these findings point out that the initial air content in the fresh state is quite susceptible to changes with time. It immediately explains why there is almost never an exact match between the initial air content in the fresh state and the air content in the hardened state. Literature search shows that many parameters (cement fineness, presence of finely divided materials, slump, temperature, mixer type, mixing time, transportation, consolidation, pumping, etc.) can influence the effectiveness of the air entrainment [34,35].

Additional mixing of the concrete normally tends to increase the fresh air content because it can induce a post-activation of the fatty acid/polyglycol based AEA (mechanism 1). An additional air entraining effect may also come from the polycarboxylic ether-based superplasticizer. This type of SP contains a defoamer to compensate for the air entraining capacities of the side chains on the comb like SP molecules. These defoamers are known to be active for only a limited period of time. As a result, they cannot prevent additional air entrainment by the SP side chains forever (mechanism 2). These two mechanisms may very well explain the evolution in air content for mixtures T(0.45)A, F(2)50A and F(2)50A-2.

The question remains why the fresh air content of F(1)50A and F(1)50A-2 decreased with time. Now, it has been reported that the presence of finely divided materials such as fly ash can be held responsible for a reduced air content. According to Dolch [35], there is a twofold explanation for this. First of all, fine fractions tend to "bind" more of the mix water because of the fact that it coats their larger surface areas. As a consequence, the water cannot be part of the air bubble generating and stabilizing process. Secondly, increased solid surface area may adsorb molecules of the AEA and render them unusable in the air entrainment process. The results obtained in this research indicate that these findings can also hold true for HVFA concrete, especially when the fly ash is very fine. The fact that fly ash F(1) (45 μm fineness: 13.2% retained) was much finer than fly ash F(2) (45 μm fineness: 26.6% retained), can explain the better performance of the AEA in combination with fly ash F(2). According to Du and Folliard [34], the carbon containing portions of fly ash are also thought to be highly adsorptive. LOI – an indicator for this carbon content, although sometimes questioned [36] – was quite similar for the two studied fly ashes (Table 2: 4.8% and 4.4%). Thus, this phenomenon probably does not explain the difference in AEA stability between F(1)50A and F(2)50A.

3.7.2. Relation: AEA addition, achieved air void system and transport properties

Adding an AEA to improve the concrete's salt scaling resistance can increase the water penetrability and gas permeability of the concrete. When looking at the capillary sorption behaviour, the use of the AEA did not seem to have an important effect. When water is forced into the concrete during the vacuum saturation test, the porosities obtained for the concrete mixtures with an AEA inside are substantially higher. Mixture F(1)50A with incorporation of the finer fly ash is the only exception. Similar trends were observed during the evaluation of the concrete's gas permeability at 2 bar pressure, especially after pre-drying at 105 °C. Apparently, whenever increased (vacuum or external) pressures are applied to measure the concrete's transport properties, air entrained concrete mixtures can be considered as more accessible to water and O_2.

4. Conclusions

HVFA concrete with a total binder content of 450 kg/m^3 and a W/B ratio of 0.35 can have an acceptable deicing salt scaling resistance ($\Delta m \leqslant 1$ kg/m^2) of the cast surface when subjected to the severe accelerated salt scaling test prescribed by the applicable European standard after both 28 and 91 days of curing. To achieve this performance, the necessary AEA dosage in presence of the specific fly ashes used in this research, must be considerably higher than for OPC concrete (7.0 ml/kg binder versus 2.0 ml/kg binder). Even then, the salt scaling resistance still tended to decrease a little bit with time. Colorimetric carbonation measurements prior to the start of every salt scaling test showed no increase in carbonation depth between 28 and 91 days. Thus, carbonation cannot explain more salt scaling after 91 days. Given this tendency of having a little more salt scaling at later age, these HVFA compositions should also be subjected to the accelerated salt scaling tests at much later ages for further verification. To see whether this phenomenon also occurs under natural freeze/thaw conditions, additional field testing would also be needed.

An adequate artificially induced air void system is necessary to minimize salt scaling. Especially when the fly ash is finer, it was found that it is more difficult to maintain the initially entrained air content necessary for an adequate air void system in hardened state. As a consequence, a sole measurement of the air content in the fresh state after 15 min is insufficient. It is recommended to measure the air content again after 60 and 120 min to evaluate its stability with time for the AEA-fly ash combination under investigation.

It is also advised to design HVFA concrete compositions in accordance with the higher air content requirements (min. 6–7%) imposed by ACI 201.2R [6] instead of the 4% and 5% air contents proposed by NBN EN 206-1 [4] and NBN B 15-001 [5], respectively. This way, the paste-to-air ratio necessary for an adequate air void system (18–20%, cf. [29,30]) is also ensured.

The combined implementation of the time dependent monitoring of the air content and the higher air content requirements would ensure that the amount of air entrained with an AEA in the presence of fly ash is enough. However, it remains unsure whether its applicability is achievable in practice.

With respect to the concretes' transport properties, it was found that the presence of the artificial air bubbles increases the permeable porosity (as measured with water sorption under vacuum) as well as the apparent gas permeability coefficient significantly. Both properties were obtained from an accelerated test that involves an external pressure. The differences were observed both after sample preconditioning at 40 °C and 105 °C and they are applicable to the OPC and HVFA concrete mixtures that were investigated in this research. It indicates that AEA additions can affect the durability performance (e.g. resistance to steel corrosion) of these concrete mixtures in a negative way. During a natural capillary sorption test on the other hand, no significant differences in the 14 days capillary water uptake could be observed between the non-air entrained and the air entrained batches of each concrete mixture.

Finally, it should be noted that increasing the pre-drying temperature to 105 °C tends to change the ranking between the OPC and HVFA concrete mixtures with respect to their 14 days capillary water uptake. Pre-drying at 105 °C also tends to amplify the difference in apparent gas permeability coefficient between the non-air entrained and the corresponding air entrained concrete mixtures. Therefore, we recommend pre-drying at 40 °C instead of at 105 °C.

References

[1] Malhorta VM, Mehta PK. High performance, high-volume fly ash concrete: materials, mixture proportioning, properties, construction practice, and case histories. 2nd ed. Ottawa: Supplementary Cementing Materials for Sustainable Development Inc.; 2005.
[2] ASTM C672-03. Standard test method for scaling resistance of concrete surfaces exposed to deicing chemicals. West Conshohocken: ASTM International; 2003.
[3] NBN EN 1339. Concrete paving flags – requirements and test methods. Brussels: CEN; 2003.
[4] NBN EN 206-1. Concrete – Part 1: specification, performance, production and conformity. Brussels: European Committee for Standardization; 2000.
[5] NBN B15-001. Supplement to NBN EN 206–1 – concrete – specification, performance, production and conformity. Brussels: BIN; 2004.
[6] ACI 201.2R. Guide to durable concrete, Reported by ACI Committee 201. Farmington Hills: American Concrete Institute; 2008.
[7] ASTM C457-10a. Standard test method for microscopical determination of parameters of the air-system in hardened concrete. West Conshohocken: ASTM International; 2010.
[8] Lammertijn S, De Belie N. Porosity, gas permeability, carbonation and their interaction in high-volume fly ash concrete. Mag Concr Res 2008;60(7):535–45.
[9] NBN EN 450-1+A1. Fly ash for concrete – Part 1: definitions, specifications and conformity criteria. Brussels: CEN; 2008.
[10] Audenaert K. Transport mechanisms of self-compacting concrete related to carbonation and chloride penetration. PhD thesis. Ghent, Ghent University, 2006 (in Dutch).
[11] Boel V, Audenaert K, De Schutter G. Gas permeability and capillary porosity of self-compacting concrete. Mater Struct 2008;41(7):1283–90.
[12] Thomas JJ, Jennings HM, Allen AJ. The surface area of hardened cement pastes as measured by various techniques. Concr Sci Eng 1999;1(1):45–64.
[13] Jennings HM. A model for the microstructure of calcium silicate hydrate in cement paste. Cem Concr Res 2000;30(1):101–16.
[14] Baroghel-Bouny V. Water vapour sorption experiments on hardened cementitious materials. Part I: essential tool for analysis of hygral behaviour and its relation to pore structure. Cem Concr Res 2007;37(3):414–37.

[15] Lothenbach B, Matschei T, Möschner G, Glasser FP. Thermodynamic modelling of the effect of temperature on the hydration and porosity of Portland cement. Cem Concr Res 2008;38(1):1–18.
[16] Jakobsen UH, Pade C, Thaulow N, Brown D, Sahu S, Magnusson O, et al. Automated air void analysis of hardened concrete – a round robin study. Cem Concr Res 2006;36(8):1444–52.
[17] Zhang DS. Air entrainment in fresh concrete with PFA. Cem Concr Compos 1996;18(6):409–16.
[18] Van den Heede P, Gruyaert E, De Belie N. Transport properties of high-volume fly ash concrete: capillary water sorption, water sorption under vacuum and gas permeability. Cem Concr Compos 2010;32(10):749–56.
[19] NBN B15-217. Concrete testing – capillary absorption test. Brussels: BIN; 1984 (in Dutch).
[20] ASTM C 1585-04e. Standard test method for measurement of rate of absorption of water by hydraulic-cement concretes. West Conshohocken: ASTM; 2007.
[21] ASTM C1202-05. Standard test method for electrical indication of concrete's ability to resist chloride ion penetration. West Conshohocken: ASTM; 2005.
[22] NBN B05-201. Resistance of materials to freezing – water absorption by capillarity. Brussels: BIN; 1976 (in Dutch).
[23] ASTM C642-06. Standard test method for density, absorption, and voids in hardened concrete. West Conshohocken: ASTM; 2006.
[24] Recommended test methods for measuring parameters associated to durability. Proc. of Journées Techniques AFPC-AFREM "Durabilité des Bétons". Toulouse: LMDC; 1998 (in French).
[25] SN 505 262/1. Construction en Béton – spécifications complémentaires. Zurich: Société des ingénieurs et des architectes; 2003.
[26] RILEM TC 116-PCD: Permeability of concrete as a criterion of its durability. Mater Struct 1999;32(217):174–9.
[27] Boel V. Microstructure of self-compacting concrete related to gas permeability and durability aspects. PhD thesis. Ghent, Ghent University, 2006 (in Dutch).
[28] Klinkenberg LJ. The permeability of porous media to liquids and gases. API: Drilling and Production Practice; 1941. p. 200–213.
[29] Pinto RCA, Hover KC. Frost and scaling resistance of high-strength concrete. RD122. Skokie: Portland Cement Association; 2001.
[30] Mielenz RC, Wolkodoff VE, Backstrom JE, Burrows RH. Origin, evolution, and effects of the air void system in concrete. Part 4 – the air void system in job concrete. ACI J Proc 1958;55(10):507–17.
[31] St. John D, Poole AW, Sims I. Concrete petrography, A handbook of investigative techniques. London: Arnold Publishers; 1998.
[32] Sommer H. The precision of the microscopical determination of the air-void system in hardened concrete. ASTM, Cem Concr Aggr 1979;1(2):49–55.
[33] Valenza II JJ, Scherer GW. A review of salt scaling: I. Phenomenology. Cem Concr Res 2007;37(7):1007–21.
[34] Du L, Folliard KJ. Mechanisms of air entrainment in concrete. Cem Concr Res 2005;35(8):1463–71.
[35] Dolch WL. Air-entraining admixtures. In: Ramachandran VS, editor. Concrete admixtures handbook: properties, science, and technology. Ottawa: National Research Council Canada; 1996. p. 518–57.
[36] Hill RL, Sarkar SL, Rathbone RF, Hover JC. An examination of fly ash carbon and its interactions with air entraining agent. Cem Concr Res 1997;27(2):193–204.